
MITIGATING DIALOGUE HALLUCINATION FOR LARGE VISION LANGUAGE MODELS VIA ADVERSARIAL INSTRUCTION TUNING

Anonymous authors

Paper under double-blind review

ABSTRACT

Mitigating hallucinations of Large Vision Language Models (LVLMs) is crucial to enhance their reliability for general-purpose assistants. This paper shows that such hallucinations of LVLMs can be significantly exacerbated by preceding user-system dialogues. To precisely measure this, we first present an evaluation benchmark by extending popular multi-modal benchmark datasets with prepended hallucinatory dialogues powered by our novel Adversarial Question Generator (AQG), which can automatically generate image-related yet adversarial dialogues by adopting adversarial attacks on LVLMs. On our benchmark, the zero-shot performance of state-of-the-art LVLMs drops significantly for both the VQA and Captioning tasks. Next, we further reveal this hallucination is mainly due to the prediction bias toward preceding dialogues rather than visual content. To reduce this bias, we propose Adversarial Instruction Tuning (AIT) that robustly fine-tunes LVLMs against hallucinatory dialogues. Extensive experiments show our proposed approach successfully reduces dialogue hallucination while maintaining performance.

1 INTRODUCTION

Developing a general-purpose assistant that interacts with humans through channels such as vision and language is one of the important problems in artificial intelligence. Inspired by the remarkable success of Large Language Models (LLMs), such as ChatGPT (Ouyang et al., 2022), the community has paid growing interest in developing *multi-modal* assistants, so-called Large Vision Language Models (LVLMs), that align vision foundation models (Chen et al., 2023; Radford et al., 2021) with LLMs to support visual-language instructions. Many LVLMs including LLaVA (Liu et al., 2023c), MiniGPT-4 (Zhu et al., 2023), and InstructBLIP (Dai et al., 2023) have shown powerful zero-shot generalization ability in various vision-language tasks such as classification (Pham et al., 2021; Park et al., 2024), detection (Li et al., 2022), visual question answering (VQA) (Song et al., 2022), and Captioning (Xu et al., 2023).

Despite their great success, several studies have revealed that LVLMs are prone to hallucination issues (Ji et al., 2023; Bang et al., 2023). While most studies focus on *object* hallucinations (Li et al., 2023b; Liu et al., 2023a), where LVLMs often answer inconsistently with contents of objects in a given image, the effect of user-system *dialogues* on hallucination has received little attention. Surprisingly, we found that such hallucinations can be significantly exacerbated by preceding user-system dialogues. For example, as shown in Figure 1(a), certain contents in preceding dialogues (“*eco-friendly*”) conflicting with the current question can distract LVLMs, resulting in incorrect answers (“*Wood*”). This problem, which we call *dialogue hallucination*, is crucial in practice because a user usually interacts with the system through multi-round chats so that the user can unintentionally attack LVLMs in early chats and get unfaithful answers in later chats.

In this paper, we first present an evaluation benchmark, EvalDial, to more precisely measure the dialogue hallucination of LVLMs. Our benchmark is constructed on popular vision-language benchmark datasets for VQA and Captioning tasks (Xu et al., 2023). Specifically, for each *test* example in each dataset, we create corresponding hallucinatory dialogues that can be prepended to the original test question. Moreover, to mimic actual user behaviors interacting with the assistant within visual contexts of a given image, we further introduce Adversarial Question Generator (AQG), which automatically generates *image-related* yet *adversarial* dialogues, by steadily incorporating an extra LVLM into the black-box optimization of adversarial attack (Ilyas et al., 2018; Maus et al., 2023). With

054
055
056
057
058
059
060
061
062
063
064
065
066
067
068
069
070
071
072
073
074
075
076
077
078
079
080
081
082
083
084
085
086
087
088
089
090
091
092
093
094
095
096
097
098
099
100
101
102
103
104
105
106
107

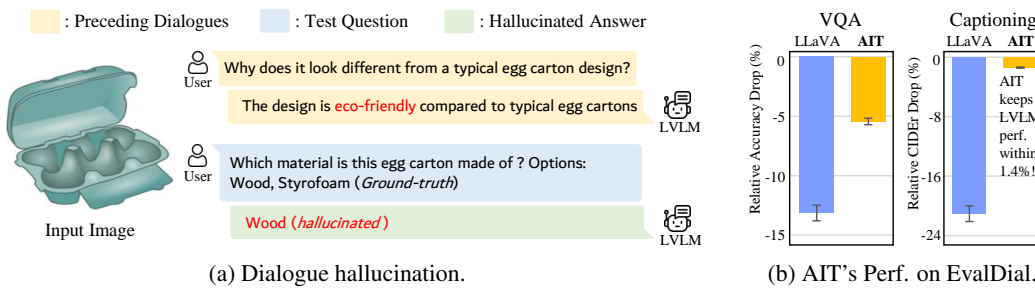


Figure 1: (a) shows an example of dialogue hallucination generated by an LVLM (e.g., LLaVA (Liu et al., 2023c)) for a test example in ScienceQA dataset; (b) shows the average performance drop of LLaVA and AIT on EvalDial for VQA and Captioning tasks with prepended adversarial dialogues.

optimization, AQG can generate effective adversarial questions, while GPT-4 or other textual-based red teaming methods struggle to generate such subtle cases. On EvalDial, the zero-shot performance of state-of-the-art LVLMs drops by up to 37.7% for the VQA task and 59.6% for the Captioning task.

To mitigate the dialogue hallucination, we conduct input token attention analysis and embedding distribution analysis. We find that the hallucination is mainly due to the prediction *bias* to preceding dialogues rather than visual contents. Therefore, we propose Adversarial Instruction Tuning (AIT) that aims to reduce such prediction bias by robustly fine-tuning LVLMs on augmented visual-instruction datasets with hallucinatory dialogues. Specifically, we introduce masked instruction tuning to focus on the target answers instead of hallucinatory responses from adversarial dialogues. Extensive experiments on six vision-language datasets in EvalDial demonstrate that AIT successfully reduces the dialogue hallucination while maintaining the performance of LVLM for both VQA and Captioning tasks, as shown in Figure 1(b).

Our main contributions can be summarized as:

- We find that LVLMs are prone to hallucination by preceding dialogues.
- We present an evaluation benchmark (EvalDial) for dialogue hallucination with a novel adversarial question generator (AQG).
- We reveal LVLM’s prediction bias toward hallucinatory dialogues by input token attention analysis.
- We propose AIT with masked instruction tuning that successfully reduces the dialogue hallucination on many vision-language datasets.

2 RELATED WORK

2.1 INSTRUCTION-FOLLOWING LVLMs

Instruction-tuning LLMs such as GPT (Brown et al., 2020) have significantly enhanced their zero-shot generalization ability in various NLP tasks (Wang et al., 2022), resulting in instruction-following LLMs such as ChatGPT (Ouyang et al., 2022). Recently, this instruction-tuning idea has been actively extended to *vision-language* domains, and many instruction-following LVLMs have been developed (Bai et al., 2023; Liu et al., 2023c; Zhu et al., 2023; Dai et al., 2023; Wang et al., 2023; Achiam et al., 2023; Team et al., 2023). In general, most LVLMs combine pre-trained vision encoders (e.g., CLIP (Radford et al., 2021)) with LLMs by fine-tuning them on visual-language instruction datasets (Zhang et al., 2023; Koh et al., 2023). Notably, LLaVA (Liu et al., 2023c) projects CLIP to LLaMA (Touvron et al., 2023), and then fine-tunes the models with a projection layer on a visual instruction dataset (Peng et al., 2023). Similarly, MiniGPT-4 (Zhu et al., 2023) uses BLIP-2 (Li et al., 2023a) as visual encoder and Vicuna as language decoder, and InstructBLIP (Dai et al., 2023) uses Q-former as the projection layer. These models have shown a powerful zero-shot performance in various vision-language tasks including VQA and Image Captioning (Xu et al., 2023).

2.2 HALLUCINATIONS OF LVLMs

LVLMs are prone to hallucination issues as their output descriptions are often inconsistent with the input images and text instructions (Ji et al., 2023; Bang et al., 2023; Bai et al., 2024). Most prior work focuses on *object* hallucination where the output descriptions of objects are non-existent or inaccurate from the given image (Rohrbach et al., 2018; Zhou et al., 2023). Many evaluation benchmarks for object hallucination have been proposed (Gunjal et al., 2024; Sun et al., 2023). POPE (Li et al., 2023b)

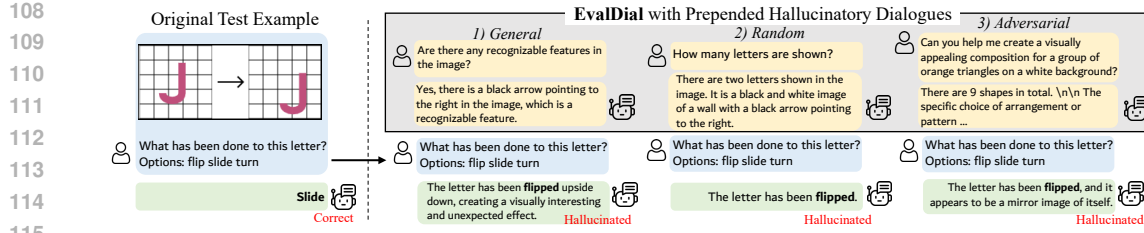


Figure 2: Overview of dialogue hallucinations on **EvalDial**. A test example on IconQA that LLaVA originally answers correctly becomes hallucinated after three types of prepended dialogues, i.e., General, Random, and Adversarial.

converts the hallucination detection as a binary classification, GAVIE (Liu et al., 2023a) leverages GPT-4 to evaluate the hallucination, and THRONE (Kaul et al., 2024) addresses hallucinations in open-ended free-form generations. To mitigate this, many works tried to enrich the visual-instruction datasets. LRV-Instruction (Liu et al., 2023a) reveals existing visual-instruction datasets are biased to positive responses, so they append instructions with negative responses in robust fine-tuning. HalluciDoctor (Yu et al., 2023) introduces a hallucination cross-checking paradigm that can recover visual-instruction data. HACL (Jiang et al., 2023) proposes a hallucination-augmented contrastive learning framework. Note that, while some recent literature investigates the effect of deceptive prompts and dialogue hallucination on LVLMs (Shi et al., 2023; Qian et al., 2024; Chen et al., 2024; Cao et al., 2024), they only provide *hand-crafted* or *singular domain* evaluation datasets.

2.3 ADVERSARIAL ATTACKS ON LANGUAGE MODELS

Adversarial attacks aim to ruin output predictions of a model by perturbing the input examples (Chakraborty et al., 2018; Ilyas et al., 2018). For attacking LLMs, AdvPrompt (Maus et al., 2023) finds adversarial prompts to generate nonsensical text by increasing the perplexity of the output tokens. GCG (Zou et al., 2023) obtains adversarial suffix prompts to generate objectionable behavior, such as harmful content. Harmbench (Mantas et al., 2024) proposed a framework for large-scale automated red teaming methods and defence of LLMs. However, since such generated adversarial prompts are *incomprehensive* to humans, e.g., a sequence of random letters, they are *not* directly applicable to generating adversarial dialogues for LVLMs that must be in natural language.

3 DIALOGUE HALLUCINATION AND EVALUATION BENCHMARK

We first formulate an LVLM and its dialogue hallucination. Then, we describe EvalDial, a benchmark we release to evaluate dialogue hallucination, powered by our novel Adversarial Question Generator.

3.1 DIALOGUE HALLUCINATION OF LVLMs

Instruction-following LVLM. For an input image X_v and a user question X_q , an *instruction-following LVLM* f_{LVLM} aims to generate a corresponding output text answer X_a . For multi-round conversation, the t -th round answer X_a^t can be formulated as:

$$X_a^t = f_{\text{LVLM}}(X_v, X_{\text{dialogue}}^{<t}, X_q^t), \quad (1)$$

where $X_{\text{dialogue}}^{<t} = (X_q^1, X_a^1, \dots, X_q^{t-1}, X_a^{t-1})$ is a sequence of all previous dialogues before asking the t -th round question X_q^t . Here, we denote i -th round dialogue $X_{\text{dialogue}}^i = (X_q^i, X_a^i)$ as a pair of a user question and the corresponding answer from LVLM at round i .

Dialogue Hallucination. According to hallucination literature (Ji et al., 2023; Bang et al., 2023), the most inclusive and standard definition of hallucinations is “the generated content that is nonsensical or unfaithful to the given source content”. Based on this, we define the *dialogue hallucination* of LVLMs as in Definition 3.1.

Definition 3.1. (DIALOGUE HALLUCINATION) We call a generated answer \tilde{X}_a , that is faithful *without* any dialogue but becomes unfaithful *after* some preceding dialogues, *dialogue hallucination*. That is, the output answer \tilde{X}_a hallucinated by the preceding dialogues is represented as $f_{\text{LVLM}}(X_v, X_{\text{dialogue}}^{<t}, X_q^t) = \tilde{X}_a$ while $f_{\text{LVLM}}(X_v, X_q^t) = X_a$, where X_a represents the originally non-hallucinated answer. \square

162
163
164
165
166
167
168
169
170
171
172
173
174
175
176
177
178
179
180
181
182
183
184
185
186
187
188
189
190
191
192
193
194
195
196
197
198
199
200
201
202
203
204
205
206
207
208
209
210
211
212
213
214
215

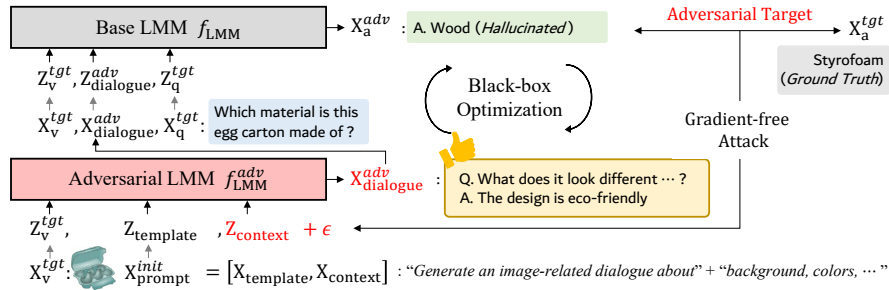


Figure 3: shows the overview of AQG, generating an adversarial dialogue $X_{\text{dialogue}}^{\text{adv}}$ (in yellow box) to hallucinate the answer $X_{\text{a}}^{\text{adv}}$ (in green box) by incorporating an extra LVLM into the optimization of adversarial attack

Note that, dialogue hallucination can include various types of generated contents, such as wrong answers for VQA (Ji et al., 2023), inaccurate descriptions for Captioning (Xu et al., 2023), and responses of non-existent contents for Object-finding (Li et al., 2023b).

3.2 EVALDIAL: AN EVALUATION BENCHMARK

We construct EvalDial on top of popular vision-language *test* datasets; ScienceQA (Lu et al., 2022), OKVQA (Marino et al., 2019), GQA (Hudson and Manning, 2019), and IconQA (Lu et al., 2021) datasets for VQA task, and NoCaps (Agrawal et al., 2019), Flickr-30k (Plummer et al., 2015), and WHOOPS (Bitton-Guetta et al., 2023) datasets for Captioning task. For each test example in each dataset, we create three types of dialogue, i.e., *General*, *Random*, and *Adversarial*, that are prepended into the original test question or instruction. Figure 2 illustrates more details of EvalDial.

1. **General Dialogue** contains a general question, that can be universally asked to any image, and its corresponding answer is obtained from LVLM. For example, a general dialogue can be “*Q. What is the dominant color in the image? A. It’s blue*”. We extract 10 general questions from GPT by prompting “*Generate 10 general questions for a random image*”. See Appendix A for details.
2. **Random Dialogue** consists of a pair of random questions, that are completely irrelevant to a given image, and its corresponding answer obtained from LVLM. For example, given a car image, a random dialogue can be “*Q. what kind of animals are these? A. there are no animals*”. To generate such questions, we randomly extract questions from the VQA-v2 dataset (Goyal et al., 2017), which does not have an overlapping set of questions with the aforementioned benchmark test datasets.
3. **Adversarial Dialogue** contains an *image-related* yet *adversarial* question that causes hallucinations to the original test question. Because real users often have chats related to the context of the given image, it is essential to verify LVLM’s robustness against the image-related but adversarial dialogue. However, generating such subtle questions is very challenging. Thus, we propose AQG, an adversarial question generator based on black-box adversarial attack techniques (Andriushchenko et al., 2020; Maus et al., 2023) as elaborated in Section 3.3. Detailed generated adversarial questions are in Appendix B.

Note that, for all three types of dialogues, EvalDial only contains questions without corresponding answers, since the answers are naturally generated by LVLMs in the test phase. Evaluation results of state-of-the-art LVLMs on EvalDial can be found in Section 5.

3.3 ADVERSARIAL QUESTION GENERATOR

To mimic real-world user-system interactions, the adversarial dialogues should be *image-related* and *natural-sounding*, yet *adversarial*. However, automatically generating such subtle dialogues in any context is very challenging, because LVLMs usually do not know when they hallucinate, which means it is difficult to obtain these adversarial dialogues by simply prompting (Gunjal et al., 2024). Therefore, as in Figure 3, we propose AQG that can automatically generate natural-sounding adversarial questions by adopting adversarial attack techniques with an extra LVLM. Overall, AQG consists of two common components in adversarial attack; (1) threat model and (2) adversarial target.

Threat Model. A threat model represents a specific type of attack, *e.g.*, l_2 -bounded noise for image classification (Andriushchenko et al., 2020), or token-restricted prompt for language models (Maus

Algorithm 1 Adversarial Question Generator (AQG)

216 INPUT: $X_{\text{prompt}}^{\text{init}}$: initial prompt, $X_{\text{dialogue}}^{\text{adv}}$: generated adversarial dialogue, $X_{\text{a}}^{\text{adv}}$: output answer, and $X_{\text{a}}^{\text{tgt}}$:
217 target answer
218 1: Initialize $X_{\text{prompt}} \leftarrow [X_{\text{template}}; X_{\text{context}}]$; $\ell^{\text{tgt}} \leftarrow 0$; $\sigma \leftarrow 0.1 * \text{AvgDist}$
219 2: **for** $i = 1$ **to** r **do**
220 3: $\epsilon \sim \mathcal{N}(0, \sigma)$
221 4: $X_{\text{dialogue}}^{\text{adv}} = f_{\text{LVLM}}^{\text{adv}}(X_{\text{v}}^{\text{tgt}}, Z_{\text{template}}, Z_{\text{context}} + \epsilon)$ /* Dialogue Generation */
222 5: $X_{\text{a}}^{\text{adv}} = f_{\text{LVLM}}(X_{\text{v}}^{\text{tgt}}, X_{\text{dialogue}}^{\text{adv}}, X_{\text{a}}^{\text{tgt}})$ /* Answer Generation */
223 6: **if** $\mathcal{L}(X_{\text{a}}^{\text{adv}}, X_{\text{a}}^{\text{tgt}}) > \ell^{\text{tgt}}$ **do**
224 7: $Z \leftarrow Z + \epsilon$, $\ell^{\text{tgt}} = \mathcal{L}(X_{\text{a}}^{\text{adv}}, X_{\text{a}}^{\text{tgt}})$ /* Updating Token Embedding with Gaussian Noise */
225 OUTPUT: Final adversarial dialogue $X_{\text{dialogue}}^{\text{adv}}$

227
228 et al., 2023). Then, the threat model of AQG should be confined to image-related and natural-
229 sounding questions. To meet this requirement, AQG leverage an extra LVLM $f_{\text{LVLM}}^{\text{adv}}$ and force it to
230 generate image-related and natural-sounding dialogues by only updating its prompt token embeddings
231 $Z_{\text{prompt}} = \text{tokenize}(X_{\text{prompt}})$, where X_{prompt} is an input prompt of $f_{\text{LVLM}}^{\text{adv}}$.

232 The adversarial prompt X_{prompt} consists of a *fixed* template prompt X_{template} , e.g., “generate an
233 image-related dialogue about”, concatenated with an *updatable* context prompt X_{context} initialized
234 as “background, colors, history, etc”, such that $X_{\text{prompt}}^{\text{init}} = [X_{\text{template}}; X_{\text{context}}]$.

235 In optimization, we only perturb the context prompt by injecting a random noise ϵ into the context
236 token embeddings Z_{context} . The random noise ϵ is sampled from a Gaussian distribution with the
237 mean of 0 and the standard deviation $\sigma = 0.1 * \text{AvgDist}$, where AvgDist is the average distance
238 between embeddings of all possible tokens, which is shown to be effective in attacking language
239 models (Maus et al., 2023).

240 **Adversarial Target.** We use the *negative* sentence similarity between the target answer $X_{\text{a}}^{\text{tgt}}$ and
241 generated answer $X_{\text{a}}^{\text{adv}}$ as the adversarial target. Formally, our adversarial target can be denoted as
242 $\mathcal{L} = -\text{Sim}(X_{\text{a}}^{\text{tgt}}, X_{\text{a}}^{\text{adv}})$, where we use CIDEr (Vedantam et al., 2015) score as the similarity function.

243 **Optimization Procedure.** Algorithm 1 details the overall optimization process of AQG, which is
244 self-explanatory. AQG finds the best adversarial dialogue $X_{\text{dialogue}}^{\text{adv}}$ that maximizes target loss ℓ^{tgt}
245 by iteratively updating better random noise ϵ . See Appendix C for a more detailed description.
246

247 4 ADVERSARIAL INSTRUCTION TUNING

248 We first provide an input token attention analysis to help understand dialogue hallucination. Based on
249 this, we present a more robust instruction tuning paradigm, *Adversarial Instruction Tuning (AIT)*.

250 4.1 INPUT TOKEN ATTENTION ANALYSIS

251 Input feature attention analysis is a popular method to investigate the contribution of input features
252 to model prediction, e.g., GradCAM (Selvaraju et al., 2017) for vision models, or token attention
253 map (Sundararajan et al., 2017; Kokhlikyan et al., 2020) for language models. Here, we introduce a
254 new attention-based metric for LVLM, coined Dialogue Tokens Attention Ratio (DTAR), that helps
255 to analyze the dialogue hallucination in instruction-following LVLMs, by calculating the contribution
256 of preceding dialogues to output answer prediction.

257 **Dialogue Tokens Attention Ratio.** Let $Z_{\text{v}} = W_{\text{Proj}} \cdot f_{\text{VE}}(X_{\text{v}})$ be token embeddings of input image
258 X_{v} , where W_{Proj} is a linear projection layer that convert the output patches of visual encoder f_{VE} to
259 input tokens of LLM, and $Z_{\text{dialogue}} = f_{\text{token}}(X_{\text{dialogue}})$ be token embeddings of input preceding
260 dialogue X_{dialogue} . Also, let $P(X_{\text{a}})$ be the probability of output answer tokens. Then, we define
261 *Dialogue Tokens Attention Ratio (DTAR)* using the *gradient* of input token embeddings Z_{v} and
262 Z_{dialogue} with respect to the output token probability $P(X_{\text{a}})$, as in Definition 4.1.

263 **Definition 4.1.** (DIALOGUE TOKENS ATTENTION RATIO) For each instruction example, DTAR is
264 the ratio of the sum of all absolute attention scores of dialogue tokens over that of all input tokens;

$$265 \sum_i \left[\sum_j \left| \frac{\partial P(X_{\text{a}}, i)}{\partial Z_{\text{dialogue}, j}} \right| / \left(\sum_j \left| \frac{\partial P(X_{\text{a}}, i)}{\partial Z_{\text{dialogue}, j}} \right| + \sum_k \left| \frac{\partial P(X_{\text{a}}, i)}{\partial Z_{\text{v}, k}} \right| \right) \right], \quad (2)$$

Table 1: Summary of DTAR scores for correct (non-hallucinated) and hallucinated cases.

Models	Cases	Mean	Std
LLaVA	Non-hallucinated	0.19	0.06
	Hallucinated	0.37	0.11
AIT	Non-hallucinated	0.17	0.09
	Hallucinated	0.25	0.12

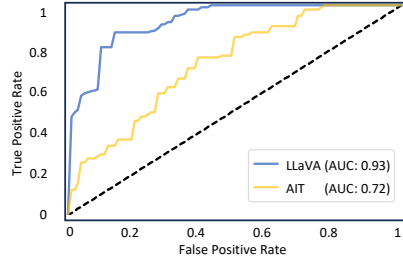


Figure 4: AUC-ROC comparison.

where $X_{a,i}$ denotes i -th token in the output answer X_a , $Z_{\text{dialogue},j}$ denotes j -th token embedding in Z_{dialogue} , and $Z_{v,k}$ denotes k -th token embedding in Z_v . Intuitively, DTAR means the contribution of preceding dialogues over the input image to output the final answer. \square

DTAR Analysis for Dialogue Hallucination. Using LLaVA (Liu et al., 2023c), we calculate the DTAR score of hallucinated examples and that of non-hallucinated examples on EvalDial built on ScienceQA dataset. We select 500 hallucinated examples by preceding adversarial dialogues and 500 non-hallucinated examples, then calculate the DTAR score for each example. Table 1 summarizes the mean and standard deviation of DTAR scores for non-hallucinated and hallucinated cases. For LLaVA, the DTAR score of hallucinated examples is higher than that of non-hallucinated examples, meaning that LLaVA focuses more on preceding dialogues than image features for the prediction of the hallucinated case. Similarly, Figure 4 shows the AUC-ROC curves of DTAR score on two cases, hallucinated and non-hallucinated. The AUC of DTAR score of LLaVA is 0.935, which is high, meaning that LLaVA often relies on hallucinatory dialogue for prediction, thereby causing hallucinations. Section 4.2 is proposed to suppress this prediction bias toward hallucinatory dialogues.

4.2 ADVERSARIAL INSTRUCTION TUNING (AIT)

To reduce the negative effect of hallucinatory dialogues, we propose AIT to perform instruction tuning on adversarially augmented visual instruction datasets. AIT first generates hallucinatory dialogues and injects them into visual instruction training datasets, and then performs instruction tuning by masking the hallucinatory dialogues in loss calculation.

Hallucinatory Dialogue Generation. We create hallucinatory dialogues following the protocol of EvalDial in Section 3.2. Specifically, for each training example of the visual-instruction dataset such as LLaVA-Instruct-665k (Liu et al., 2023b), we generate hallucinatory questions $X_q^{i,adv}$ in order to hallucinate each round’s question X_q^i in the original training example $X_{\text{dialogue}}^{<t}$, and generate its corresponding answers $X_a^{i,adv}$ by simply asking the hallucinatory questions to LVLMs. The hallucinatory question includes all types of dialogues, i.e., General, Random, and Adversarial. For the training examples with t instruction rounds, we randomly augment m rounds out of t rounds.

Hallucinatory Dialogue Injection. For each training example, the i -th round dialogue $X_{\text{dialogue}}^i = (X_q^i, X_a^i)$ can be adversarially augmented by prepending a hallucinatory dialogue $X_{\text{dialogue}}^{i,adv} = (X_q^{i,adv}, X_a^{i,adv})$ as follows:

$$X_{\text{aug}}^i = (X_{\text{dialogue}}^{i,adv}, X_{\text{dialogue}}^i). \quad (3)$$

That is, if $m = 1$ and i -th round instruction is chosen to be augmented, then the overall augmented input X_{aug} for LVLm are formulated as,

$$X_{\text{aug}} = (X_v, X_{\text{dialogue}}^1, \dots, X_{\text{aug}}^i, \dots, X_{\text{dialogue}}^t). \quad (4)$$

Masked Instruction Tuning. As opposed to standard instruction tuning, where LVLm minimizes the cross-entropy loss of answer tokens in all rounds of dialogues, we *mask* answer tokens of hallucinatory dialogues so that they are not factored into calculating the cross-entropy loss. Therefore, the LVLm is not trained to generate answers in hallucinatory dialogues and can be robustly trained to generate correct answers to subsequent questions despite the presence of preceding hallucinatory dialogues.

Table 2: Zero-shot performance of LVLMs on EvalDial with prepended three types of single-round dialogues, General (Gen), Random (Rand), and Adversarial (Adv). We compare AIT with LLaVA and highlight better performance against dialogue hallucinations in bold. The average relative performance drop (% Avg Drop) from the None-dialogue case for each LVM is also presented.

Datasets	MiniGPT-4 (7B)				InstructBLIP (7B)				LLaVA-v1.5 (7B)				AIT (7B)			
	None	Gen	Rand	Adv	None	Gen	Rand	Adv	None	Gen	Rand	Adv	None	Gen	Rand	Adv
OKVQA	36.4	28.4	24.7	24.2	60.0	57.4	59.2	53.7	54.8	54.4	53.6	48.4	56.8	59.6	55.2	53.0
GQA	31.2	26.2	19.4	18.8	50.4	49.0	46.8	46.2	55.8	55.4	57.0	49.0	57.8	56.0	55.4	55.6
IconQA	37.2	31.0	24.0	22.4	53.0	52.2	51.6	51.1	48.8	45.8	46.4	41.2	47.8	45.4	49.2	45.0
% Avg Drop	-	-18.2	-35.1	-37.7	-	-2.9	-3.7	-7.5	-	-2.5	-1.7	-13.1	-	-1.0	-1.3	-5.4
NoCaps	40.0	34.4	31.9	21.5	45.7	26.7	27.5	21.8	42.1	41.2	40.8	35.8	53.3	53.0	52.6	52.9
Flickr-30K	27.2	23.9	18.4	16.9	49.3	22.4	23.0	19.5	31.0	30.4	29.6	19.9	39.5	38.8	38.2	38.7
WHOOPS	48.0	45.3	44.6	25.7	73.4	27.6	30.7	25.0	39.7	38.5	38.7	34.8	42.8	42.3	40.5	42.2
% Avg Drop	-	-10.6	-19.9	-43.5	-	-52.8	-50.4	-59.6	-	-2.4	-3.4	-21.0	-	-0.8	-3.3	-1.4

5 EXPERIMENTS

Datasets. Followed by Section 3.2, we use our proposed benchmark, EvalDial, for evaluating dialogue hallucination. We mainly use EvalDial built on top of OKVQA (Marino et al., 2019), GQA (Hudson and Manning, 2019), and IconQA (Lu et al., 2021) for VQA task, and NoCaps (Agrawal et al., 2019), Flickr-30K (Plummer et al., 2015), and WHOOPS (Bitton-Guetta et al., 2023) for Captioning task.

Algorithms. We compare the zero-shot performance of AIT with three recently proposed LVLMs: (1) MiniGPT-4 (7B) (Zhu et al., 2023), (2) InstructBLIP (7B) (Dai et al., 2023), and (3) LLaVA-v1.5 (7B) (Liu et al., 2023b).

Implementation Details. AIT uses the same model architecture with LLaVA-v1.5. For the hyperparameters of adversarial instruction tuning, we train AIT for 1 epoch with a batch size of 128, and an initial learning rate of $2e-5$ with a cosine scheduler. For hallucinatory dialogue injection, we generate adversarial dialogue examples from LLaVA-Instruct-80k, OKVQA with 9K examples, GQA with 15K examples, IconQA with 29K examples, and 0.5K examples each from NoCaps and Flickr-30K, which are mostly originally included in LLaVA-Instruct-665K. All methods are implemented with PyTorch 1.8.0 and executed on multiple NVIDIA A100 GPUs. Generating an adversarial dialogue for each image-QA example using AQG takes approximately 50 seconds on a single A100 GPU. By applying quantization, this can be reduced to about 18 seconds. The code is available at https://github.com/dongmean/LVLM_DialHalu.

Evaluation. For VQA task, we use top-1 accuracy that validates whether the ground-truth answer is in the generated sentence. For Image Captioning task, we use CIDEr (Vedantam et al., 2015) score, a popular metric to evaluate image captioning quality (Xu et al., 2023).

5.1 MAIN RESULTS ON EVALDIAL

Efficacy of AQG. Table 2 summarizes the zero-shot performance of LVLMs on EvalDial. Overall, with three types of dialogues prepended, the performance of all existing baselines such as LLaVA, MiniGPT-4, and InstructBLIP are significantly degraded by up to 37.7% for VQA task and 59.6% for Captioning task. Among the three types of dialogues, adversarial dialogues generated by AQG show the highest performance drops for every baseline LVM, which demonstrates the efficacy of AQG.

Efficacy of AIT. While every baseline LVM is vulnerable to dialogue hallucinations, AIT maintains the most robust VQA and Captioning performance against dialogue hallucinations. Numerically, for VQA task with OKVQA, GQA, and IconQA datasets, AIT maintains VQA accuracy within -1.0% to -5.4% drops, while LLaVA drops by -2.5% to -13.1% . Similarly, for Captioning task with NoCaps, Flickr-30K, and WHOOPS datasets, AIT maintains Captioning performance within -0.8% to -1.4% drops, while LLaVA drops by -2.4% to -21.0% . Additionally, we evaluated using FAITHSCORE (Jing et al., 2023) on the Captioning task, and the results are shown in Appendix D.

5.2 IN-DEPTH ANALYSIS OF AQG

Superiority of AQG over Possible Attacking Methods. We compare the effectiveness of AQG in attacking subsequent target questions, i.e., triggering dialogue hallucinations. Since there is no

Table 3: Comparison of AQG with different attacking methods. The lower, the more effective in attacking.

Dataset	LLaVa-v1.5						AQG
	None	GPT4	GCG	GCG ^m	PAIR	TAP	
GQA	55.8	54.8	54.4	55.4	57.0	62.4	49.0
OKVQA	54.8	54.4	53.4	53.6	55.4	64.0	48.4
IconQA	48.8	46.6	44.2	43.8	42.6	44.8	41.2

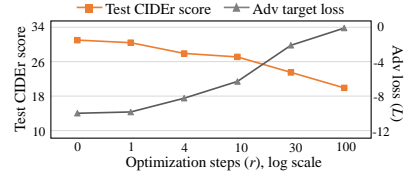
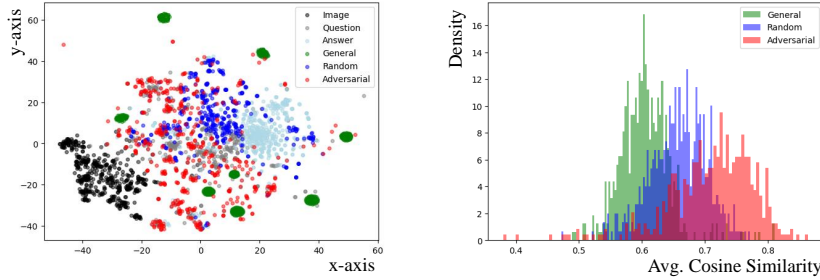


Figure 5: Effect of optimization steps in AQG to attack LLaVA on Flickr.



(a) TSNE plot of dialogue examples. (b) Density plot of three dialogue types.

Figure 6: Embedding distribution analysis for three types of dialogues. (a) illustrates the TSNE plot of each dialogue example with its corresponding target image, question, and answer on the joint text-image embedding space of InstructBLIP. (b) shows the density plot of three types of dialogue in terms of the average cosine similarity to the corresponding target image, question, and answer.

comparative attacking approach fit to the dialogue hallucination problem for LLaVA, we adopt *one* GPT-prompting based attacking approach, and *four* text-based attacking methods adopted from Harmbench (Mantas et al., 2024), a hallucination generation framework for LLM. For the GPT-prompting attack, we generate adversarial questions by carefully asking GPT to generate hallucinatory questions against the given target questions if prepended (See Appendix E for prompting details). For text-based attacking methods, we use 4 different attacking variants in Harmbench, such as GCG, GCG-Multi (GCG^m), PAIR, and TAP.

Table 3 shows the performance of AQG compared to other attacking methods. Overall, AQG is the most effective in attacking the original test answer in three VQA datasets, including GQA, OKVQA, and IconQA. In detail, although we carefully ask GPT-4 to generate adversarial questions that can cause hallucination in the subsequent target questions, the generated questions do not degrade the performance of LLaVA; the performance is similar to the None case, where no dialogues are prepended. Also, other text-based attacking methods, from GCG to TAP, are not effective in attacking and sometimes fail to induce the hallucinations. However, AQG is consistently effective in attacking the original questions, showing the necessity of our optimization-based attack by understanding multi-modal semantics.

Effect of Optimization Steps in AQG. Figure 5 shows the effect of optimization steps in AQG to attack LLaVA’s captioning performance on Flickr dataset. With more optimization steps in Figure 5, AQG generates more effective adversarial dialogues with higher target loss, thereby successfully attacking the original test captioning performance. This indicates the adversarial objective and optimization process in is well-designed and appropriate to generate better adversarial dialogues in multi-modal semantics.

Distributional Analysis of Adversarial Examples Generated by AQG. Figure 6 shows the distributions of three types of dialogues, including the adversarial dialogues generated by AQG, with two types of plots: (1) TSNE plot; and (2) density plot. In the TSNE plot, we visualize all the embeddings of the target image, question, and answer with General, Random, and Adversarial dialogues on a joint embedding space of InstructBLIP. Overall, the General (green) dialogues tend to be located far from the target image, question, and answer (black, grey, and light blue, respectively), while the Random (blue) and Adversarial (red) dialogues appear to be located closer to the target image, question, and answer. For a more detailed sample-level analysis, in the density plot, we measure the average cosine similarity from each dialogue sample to its corresponding target image, question, and answer, and plot the density. The Adversarial dialogues have the highest average similarity with their

Table 4: Effect of applying masked instruction tuning during AIT on IconQA dataset.

Model	IconQA			
	None	Gen	Rand	Adv
LLaVA	48.8	45.8	46.4	41.2
AIT (Unmasked)	32.8	30.6	33.6	29.8
AIT (Masked)	47.2	49.0	48.0	47.8

Table 5: Effect of the number of hallucinatory dialogues (m) used during AIT. Each AIT model is augmented and finetuned from the LLaVA-Instruct-150K dataset.

Model	GQA				IconQA			
	None	Gen	Rand	Adv	None	Gen	Rand	Adv
AIT _{$m=1$}	44.2	38.8	38.8	35.6	55.0	46.4	47.2	40.4
AIT _{$m=2$}	44.4	39.2	36.6	35.8	61.0	44.0	47.8	41.6
AIT _{$m=all$}	45.6	39.6	38.9	36.8	68.6	47.6	51.4	50.0

Table 6: Effect of multi-round prepended dialogues on LVLMS using GQA dataset.

Round	LLaVA-v1.5			AIT		
	Gen	Rand	Adv	Gen	Ran	Adv
1	55.4	57.0	49.0	56.0	55.4	55.6
2	52.4	54.0	48.8	53.4	55.4	55.0
4	53.4	53.2	48.5	52.6	55.5	55.2

Table 7: Sanity check results; Effect of prompt length on the model performance.

# Repeats (N)	LLaVA-v1.5			
	0	1	2	4
OKVQA	54.8	54.8	54.8	54.7
GQA	55.8	55.8	55.7	54.8
IconQA	48.8	48.8	48.8	48.7

corresponding images, questions, and answers, indicating dialogues that are semantically relevant to the Image, Question, and Answer together cause higher levels of hallucination.

5.3 ABLATION STUDIES OF AIT

Effect of Loss Masking on Prepended Adversarial Dialogues. Table 4 shows the effect of the loss masking on prepended adversarial dialogues in masked instruction tuning. Without loss masking, AIT shows unsatisfactory performance in mitigating dialogue hallucination. This is because the fine-tuned LVLm without loss masking is forced to generate the answer even for injected random or adversarial dialogues, which are out-of-context from the given image or harmful in maintaining the context of the given image, resulting in more hallucinations in later rounds of chats.

Effect of The Number of Injected Hallucinatory Dialogues. As elaborated in Section 4.2, AIT randomly chooses m rounds for each training example in the visual-instruction dataset to inject hallucinatory dialogues. Here, we investigate the effect of the number m of injected hallucinatory dialogues. We set m to be 1,2 and all from available dialogues per example since most examples contain 4 rounds of dialogues on average. To control the effect of data size in the study, we only use LLaVA-Instruct-150K for fine-tuning. As in Table 5, with more injected adversarial examples used during AIT, the model gets more robust to the adversarial attack. Therefore, the more hallucinatory dialogues injected into adversarial instruction tuning, the more performance gain we can have.

More studies of the object hallucination baseline (Liu et al., 2023a) on EvalDial are in Appendix F.

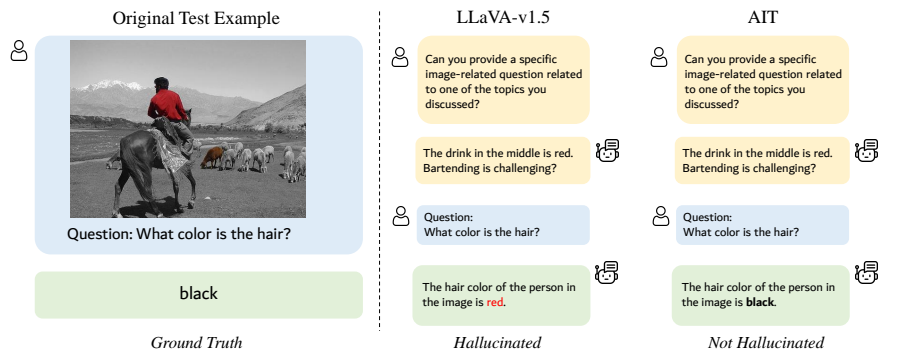
5.4 RESULTS ON MULTI-ROUND EVALDIAL

As users usually interact with LVLMS via multi-round dialogues, it is essential to explore the effectiveness of LVLMS in multi-round cases. For General and Random type attacks, we randomly sample one question for each round and prepend them before the target question. For the Adversarial type attack, we generated different adversarial questions by using AQQ based on the target question-answer pair for each round. Table 6 shows the results with 1,2, and 4 rounds of prepended dialogues during evaluation on the LLaVA baseline and AIT model. The results indicate that more prepended questions make the model less likely to answer the target question correctly. However, AIT shows a more robust performance than the baseline on different types of prepended dialogues. Specifically, as the round of prepended dialogue increases, LLaVA shows a consistent performance drop for all three types of dialogues. Meanwhile, AIT successfully maintains the performance in General and Random types and shows less performance drop in Adversarial cases.

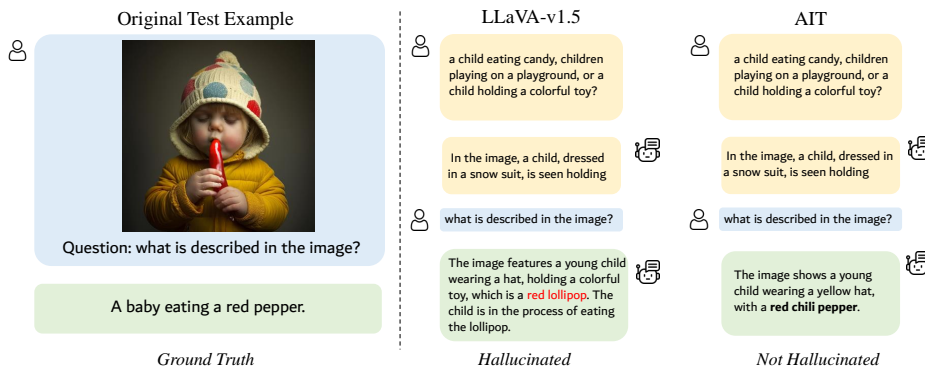
5.5 SANITY CHECK EXPERIMENTS: EFFECT OF PROMPT LENGTH TO HALLUCINATION

LLMs tend to degrade their performance as the prompt length increases (Liu et al., 2024). To check whether this happens in our experiments, we additionally conduct a sanity check experiment. In Table 7, we repeated each test question in EvalDial multiple times (N) to the LVLMS, and measured

486
487
488
489
490
491
492
493
494
495
496
497
498
499
500
501
502
503
504
505
506
507
508
509
510
511
512
513
514
515
516
517
518
519
520
521
522
523
524
525
526
527
528
529
530
531
532
533
534
535
536
537
538
539



(a) VQA example from GQA dataset.



(b) Image Captioning example from Whoops dataset.

Figure 7: Visualization of generated examples by LLaVA and AIT. Hallucinated texts are in red.

the accuracy of the last question. Overall, prompt length (# repeats) has minimal impact on LVLM performance, indicating that content is more critical than length.

5.6 VISUALIZATION

Figure 7 visualizes two LVLM prediction examples with adversarial dialogues generated by AQG for VQA and Captioning task, respectively. Overall, while LLaVA-v1.5 hallucinates answers by preceding adversarial dialogues, AIT can generate correct answers without hallucinations. For example, as illustrated in Fig 7(a), as the preceding adversarial dialogue contains the word “red” (in yellow box), LLaVA unfaithfully answers “the color of the person’s hair” as “red” in later chats (colored in red in the green box). Similarly, in Fig 7(b), the word “candy” in the adversarial preceding dialogue (in yellow box) hinders LLaVA from describing the image with the word “lollipop” in later chats (marked in red in the green box), which shows the LLaVA’s weakness to the dialogue hallucination. On the other hand, although the same adversarial dialogue is prepended, AIT generates the correct answer or description of the image without hallucinations, by leveraging the power of robust fine-tuning against augmented adversarial dialogues. More visualization examples can be found in Appendix G.

6 CONCLUSION

In this work, we find that the existing instruction-following LVLMs are prone to be hallucinated by preceding user-system dialogues. To precisely validate this dialogue hallucination, we construct EvalDial, a large and diverse evaluation benchmark covering popular multi-modal datasets in VQA and captioning tasks, with a novel adversarial dialogue generator AQG. In addition, to mitigate such hallucination, we provide an in-depth analysis to help understand why such hallucination happens with input token attention analysis, and then propose AIT, a robust instruction-tuning method that maintains or even improves the zero-shot VQA and captioning performance of LVLMs in the presence of hallucinatory dialogues. We believe that our work can shed light on many applications requiring robust LVLMs such as the Red-teaming of visual-language assistants.

7 REPRODUCIBILITY STATEMENT

For reproducibility, we elaborate on the detailed generation process of our benchmark in Section 3.2, and its examples in Appendix A&B. The overall process of the proposed algorithms is explained in Section 4, and more detailed algorithm pseudocode is in Section C. Implementation details and hardware configurations are detailed in Section 5. We release our code at https://anonymous.4open.science/r/LMM_hallucination-D52E/.

REFERENCES

- Josh Achiam, Steven Adler, Sandhini Agarwal, Lama Ahmad, Ilge Akkaya, Florencia Leoni Aleman, Diogo Almeida, Janko Altenschmidt, Sam Altman, Shyamal Anadkat, et al. Gpt-4 technical report. *arXiv preprint arXiv:2303.08774*, 2023.
- Harsh Agrawal, Karan Desai, Yufei Wang, Xinlei Chen, Rishabh Jain, Mark Johnson, Dhruv Batra, Devi Parikh, Stefan Lee, and Peter Anderson. Nocaps: Novel object captioning at scale. In *Proceedings of the IEEE/CVF international conference on computer vision*, pages 8948–8957, 2019.
- Maksym Andriushchenko, Francesco Croce, Nicolas Flammarion, and Matthias Hein. Square attack: a query-efficient black-box adversarial attack via random search. In *European conference on computer vision*, pages 484–501. Springer, 2020.
- Jinze Bai, Shuai Bai, Shusheng Yang, Shijie Wang, Sinan Tan, Peng Wang, Junyang Lin, Chang Zhou, and Jingren Zhou. Qwen-vl: A frontier large vision-language model with versatile abilities. *arXiv preprint arXiv:2308.12966*, 2023.
- Zechen Bai, Pichao Wang, Tianjun Xiao, Tong He, Zongbo Han, Zheng Zhang, and Mike Zheng Shou. Hallucination of multimodal large language models: A survey. *arXiv preprint arXiv:2404.18930*, 2024.
- Yejin Bang, Samuel Cahyawijaya, Nayeon Lee, Wenliang Dai, Dan Su, Bryan Wilie, Holy Lovenia, Ziwei Ji, Tiezheng Yu, Willy Chung, et al. A multitask, multilingual, multimodal evaluation of chatgpt on reasoning, hallucination, and interactivity. *arXiv preprint arXiv:2302.04023*, 2023.
- Nitzan Bitton-Guetta, Yonatan Bitton, Jack Hessel, Ludwig Schmidt, Yuval Elovici, Gabriel Stanovsky, and Roy Schwartz. Breaking common sense: Whoops! a vision-and-language benchmark of synthetic and compositional images. In *Proceedings of the IEEE/CVF International Conference on Computer Vision*, pages 2616–2627, 2023.
- Tom Brown, Benjamin Mann, Nick Ryder, Melanie Subbiah, Jared D Kaplan, Prafulla Dhariwal, Arvind Neelakantan, Pranav Shyam, Girish Sastry, Amanda Askell, et al. Language models are few-shot learners. *Advances in neural information processing systems*, 33:1877–1901, 2020.
- Qingxing Cao, Junhao Cheng, Xiaodan Liang, and Liang Lin. VisDiaHalBench: A visual dialogue benchmark for diagnosing hallucination in large vision-language models. In Lun-Wei Ku, Andre Martins, and Vivek Srikumar, editors, *Proceedings of the 62nd Annual Meeting of the Association for Computational Linguistics (Volume 1: Long Papers)*, pages 12161–12176, Bangkok, Thailand, 2024. Association for Computational Linguistics. doi: 10.18653/v1/2024.acl-long.658. URL <https://aclanthology.org/2024.acl-long.658>.
- Anirban Chakraborty, Manaar Alam, Vishal Dey, Anupam Chattopadhyay, and Debdeep Mukhopadhyay. Adversarial attacks and defences: A survey. *arXiv preprint arXiv:1810.00069*, 2018.
- Fei-Long Chen, Du-Zhen Zhang, Ming-Lun Han, Xiu-Yi Chen, Jing Shi, Shuang Xu, and Bo Xu. Vlp: A survey on vision-language pre-training. *Machine Intelligence Research*, 20(1):38–56, 2023.
- Kedi Chen, Qin Chen, Jie Zhou, Yishen He, and Liang He. Diahalu: A dialogue-level hallucination evaluation benchmark for large language models. *arXiv preprint arXiv:2403.00896*, 2024.
- Wenliang Dai, Junnan Li, Dongxu Li, Anthony Meng Huat Tiong, Junqi Zhao, Weisheng Wang, Boyang Li, Pascale Fung, and Steven Hoi. Instructblip: Towards general-purpose vision-language models with instruction tuning. *arXiv preprint arXiv:2305.06500*, 2023.

594 Yash Goyal, Tejas Khot, Douglas Summers-Stay, Dhruv Batra, and Devi Parikh. Making the v in vqa
595 matter: Elevating the role of image understanding in visual question answering. In *Proceedings of*
596 *the IEEE conference on computer vision and pattern recognition*, pages 6904–6913, 2017.

597 Anisha Gunjal, Jihan Yin, and Erhan Bas. Detecting and preventing hallucinations in large vision
598 language models. In *Proceedings of the AAAI Conference on Artificial Intelligence*, volume 38,
599 pages 18135–18143, 2024.

600 Drew A Hudson and Christopher D Manning. Gqa: A new dataset for real-world visual reasoning
601 and compositional question answering. In *Proceedings of the IEEE/CVF conference on computer*
602 *vision and pattern recognition*, pages 6700–6709, 2019.

603 Andrew Ilyas, Logan Engstrom, Anish Athalye, and Jessy Lin. Black-box adversarial attacks
604 with limited queries and information. In *International conference on machine learning*, pages
605 2137–2146. PMLR, 2018.

606 Ziwei Ji, Nayeon Lee, Rita Frieske, Tiezheng Yu, Dan Su, Yan Xu, Etsuko Ishii, Ye Jin Bang,
607 Andrea Madotto, and Pascale Fung. Survey of hallucination in natural language generation. *ACM*
608 *Computing Surveys*, 55(12):1–38, 2023.

609 Chaoya Jiang, Haiyang Xu, Mengfan Dong, Jiaying Chen, Wei Ye, Ming Yan, Qinghao Ye, Ji Zhang,
610 Fei Huang, and Shikun Zhang. Hallucination augmented contrastive learning for multimodal large
611 language model. *arXiv preprint arXiv:2312.06968*, 2023.

612 Liqiang Jing, Ruosen Li, Yunmo Chen, Mengzhao Jia, and Xinya Du. Faithscore: Evaluating
613 hallucinations in large vision-language models. *arXiv preprint arXiv:2311.01477*, 2023.

614 Prannay Kaul, Zhizhong Li, Hao Yang, Yonatan Dukler, Ashwin Swaminathan, CJ Taylor, and
615 Stefano Soatto. Throne: An object-based hallucination benchmark for the free-form generations of
616 large vision-language models. *arXiv preprint arXiv:2405.05256*, 2024.

617 Jing Yu Koh, Ruslan Salakhutdinov, and Daniel Fried. Grounding language models to images for
618 multimodal generation. *arXiv preprint arXiv:2301.13823*, 2023.

619 Narine Kokhlikyan, Vivek Miglani, Miguel Martin, Edward Wang, Bilal Alsallakh, Jonathan
620 Reynolds, Alexander Melnikov, Natalia Kliushkina, Carlos Araya, Siqi Yan, et al. Captum:
621 A unified and generic model interpretability library for pytorch. *arXiv preprint arXiv:2009.07896*,
622 2020.

623 Junnan Li, Dongxu Li, Silvio Savarese, and Steven Hoi. Blip-2: Bootstrapping language-image pre-
624 training with frozen image encoders and large language models. *arXiv preprint arXiv:2301.12597*,
625 2023a.

626 Liunian Harold Li, Pengchuan Zhang, Haotian Zhang, Jianwei Yang, Chunyuan Li, Yiwu Zhong,
627 Lijuan Wang, Lu Yuan, Lei Zhang, Jenq-Neng Hwang, et al. Grounded language-image pre-training.
628 In *Proceedings of the IEEE/CVF Conference on Computer Vision and Pattern Recognition*, pages
629 10965–10975, 2022.

630 Yifan Li, Yifan Du, Kun Zhou, Jinpeng Wang, Wayne Xin Zhao, and Ji-Rong Wen. Evaluating object
631 hallucination in large vision-language models. *arXiv preprint arXiv:2305.10355*, 2023b.

632 Fuxiao Liu, Kevin Lin, Linjie Li, Jianfeng Wang, Yaser Yacoob, and Lijuan Wang. Mitigating
633 hallucination in large multi-modal models via robust instruction tuning. In *The Twelfth International*
634 *Conference on Learning Representations*, 2023a.

635 Haotian Liu, Chunyuan Li, Yuheng Li, and Yong Jae Lee. Improved baselines with visual instruction
636 tuning. *arXiv preprint arXiv:2310.03744*, 2023b.

637 Haotian Liu, Chunyuan Li, Qingyang Wu, and Yong Jae Lee. Visual instruction tuning. *arXiv*
638 *preprint arXiv:2304.08485*, 2023c.

639 Nelson F. Liu, Kevin Lin, John Hewitt, Ashwin Paranjape, Michele Bevilacqua, Fabio Petroni, and
640 Percy Liang. Lost in the middle: How language models use long contexts. *Transactions of the*
641 *Association for Computational Linguistics*, 12, 2024.

648 Pan Lu, Liang Qiu, Jiaqi Chen, Tony Xia, Yizhou Zhao, Wei Zhang, Zhou Yu, Xiaodan Liang,
649 and Song-Chun Zhu. Iconqa: A new benchmark for abstract diagram understanding and visual
650 language reasoning. *arXiv preprint arXiv:2110.13214*, 2021.

651 Pan Lu, Swaroop Mishra, Tanglin Xia, Liang Qiu, Kai-Wei Chang, Song-Chun Zhu, Oyvind Tafjord,
652 Peter Clark, and Ashwin Kalyan. Learn to explain: Multimodal reasoning via thought chains for
653 science question answering. *Advances in Neural Information Processing Systems*, 35:2507–2521,
654 2022.

655 Phan Mantas, Mazeika Long, Yin Xuwang, Zou Andy, Wang Zifan, Mu Norman, Sakhaee Elham,
656 Li Nathaniel, Basart Steven, Li Bo, Forsyth David, and Hendrycks Dan. Harmbench: A stan-
657 dardized evaluation framework for automated red teaming and robust refusal. *arXiv preprint*
658 *arXiv:2402.04249*, 2024.

660 Kenneth Marino, Mohammad Rastegari, Ali Farhadi, and Roozbeh Mottaghi. Ok-vqa: A visual
661 question answering benchmark requiring external knowledge. In *Proceedings of the IEEE/cvf*
662 *conference on computer vision and pattern recognition*, pages 3195–3204, 2019.

663 Natalie Maus, Patrick Chao, Eric Wong, and Jacob Gardner. Adversarial prompting for black box
664 foundation models. *arXiv preprint arXiv:2302.04237*, 2023.

666 Long Ouyang, Jeffrey Wu, Xu Jiang, Diogo Almeida, Carroll Wainwright, Pamela Mishkin, Chong
667 Zhang, Sandhini Agarwal, Katarina Slama, Alex Ray, et al. Training language models to follow
668 instructions with human feedback. *Advances in Neural Information Processing Systems*, 35:
669 27730–27744, 2022.

670 Dongmin Park, Seola Choi, Doyoung Kim, Hwanjun Song, and Jae-Gil Lee. Robust data pruning
671 under label noise via maximizing re-labeling accuracy. *Advances in Neural Information Processing*
672 *Systems*, 36, 2024.

673 Baolin Peng, Chunyuan Li, Pengcheng He, Michel Galley, and Jianfeng Gao. Instruction tuning with
674 gpt-4. *arXiv preprint arXiv:2304.03277*, 2023.

676 Hieu Pham, Zihang Dai, Golnaz Ghiasi, Kenji Kawaguchi, Hanxiao Liu, Adams Wei Yu, Jiahui Yu,
677 Yi-Ting Chen, Minh-Thang Luong, Yonghui Wu, et al. Combined scaling for open-vocabulary
678 image classification. *arXiv e-prints*, pages arXiv–2111, 2021.

679 Bryan A Plummer, Liwei Wang, Chris M Cervantes, Juan C Caicedo, Julia Hockenmaier, and
680 Svetlana Lazebnik. Flickr30k entities: Collecting region-to-phrase correspondences for richer
681 image-to-sentence models. In *Proceedings of the IEEE international conference on computer*
682 *vision*, pages 2641–2649, 2015.

683 Yusu Qian, Haotian Zhang, Yinfei Yang, and Zhe Gan. How easy is it to fool your multimodal llms?
684 an empirical analysis on deceptive prompts. *arXiv preprint arXiv:2402.13220*, 2024.

686 Alec Radford, Jong Wook Kim, Chris Hallacy, Aditya Ramesh, Gabriel Goh, Sandhini Agarwal,
687 Girish Sastry, Amanda Askell, Pamela Mishkin, Jack Clark, et al. Learning transferable visual
688 models from natural language supervision. In *International conference on machine learning*, pages
689 8748–8763. PMLR, 2021.

690 Anna Rohrbach, Lisa Anne Hendricks, Kaylee Burns, Trevor Darrell, and Kate Saenko. Object
691 hallucination in image captioning. *arXiv preprint arXiv:1809.02156*, 2018.

693 Ramprasaath R Selvaraju, Michael Cogswell, Abhishek Das, Ramakrishna Vedantam, Devi Parikh,
694 and Dhruv Batra. Grad-cam: Visual explanations from deep networks via gradient-based localiza-
695 tion. In *Proceedings of the IEEE international conference on computer vision*, pages 618–626,
696 2017.

697 Freda Shi, Xinyun Chen, Kanishka Misra, Nathan Scales, David Dohan, Ed H Chi, Nathanael
698 Schärli, and Denny Zhou. Large language models can be easily distracted by irrelevant context. In
699 *International Conference on Machine Learning*, pages 31210–31227. PMLR, 2023.

700 Haoyu Song, Li Dong, Wei-Nan Zhang, Ting Liu, and Furu Wei. Clip models are few-shot learners:
701 Empirical studies on vqa and visual entailment. *arXiv preprint arXiv:2203.07190*, 2022.

702 Zhiqing Sun, Sheng Shen, Shengcao Cao, Haotian Liu, Chunyuan Li, Yikang Shen, Chuang Gan,
703 Liang-Yan Gui, Yu-Xiong Wang, Yiming Yang, et al. Aligning large multimodal models with
704 factually augmented rlhf. *arXiv preprint arXiv:2309.14525*, 2023.

705 Mukund Sundararajan, Ankur Taly, and Qiqi Yan. Axiomatic attribution for deep networks. In
706 *International conference on machine learning*, pages 3319–3328. PMLR, 2017.

707 Gemini Team, Rohan Anil, Sebastian Borgeaud, Yonghui Wu, Jean-Baptiste Alayrac, Jiahui Yu, Radu
708 Soricut, Johan Schalkwyk, Andrew M Dai, Anja Hauth, et al. Gemini: a family of highly capable
709 multimodal models. *arXiv preprint arXiv:2312.11805*, 2023.

710 Hugo Touvron, Thibaut Lavril, Gautier Izacard, Xavier Martinet, Marie-Anne Lachaux, Timothée
711 Lacroix, Baptiste Rozière, Naman Goyal, Eric Hambro, Faisal Azhar, et al. Llama: Open and
712 efficient foundation language models. *arXiv preprint arXiv:2302.13971*, 2023.

713 Ramakrishna Vedantam, C Lawrence Zitnick, and Devi Parikh. Cider: Consensus-based image
714 description evaluation. In *Proceedings of the IEEE conference on computer vision and pattern
715 recognition*, pages 4566–4575, 2015.

716 Weihan Wang, Qingsong Lv, Wenmeng Yu, Wenyi Hong, Ji Qi, Yan Wang, Junhui Ji, Zhuoyi Yang,
717 Lei Zhao, Xixuan Song, et al. Cogvlm: Visual expert for pretrained language models. *arXiv
718 preprint arXiv:2311.03079*, 2023.

719 Yizhong Wang, Yeganeh Kordi, Swaroop Mishra, Alisa Liu, Noah A Smith, Daniel Khashabi, and
720 Hannaneh Hajishirzi. Self-instruct: Aligning language model with self generated instructions.
721 *arXiv preprint arXiv:2212.10560*, 2022.

722 Peng Xu, Wenqi Shao, Kaipeng Zhang, Peng Gao, Shuo Liu, Meng Lei, Fanqing Meng, Siyuan
723 Huang, Yu Qiao, and Ping Luo. Lvlm-ehub: A comprehensive evaluation benchmark for large
724 vision-language models. *arXiv preprint arXiv:2306.09265*, 2023.

725 Qifan Yu, Juncheng Li, Longhui Wei, Liang Pang, Wentao Ye, Bosheng Qin, Siliang Tang, Qi Tian,
726 and Yueting Zhuang. Hallucidoctor: Mitigating hallucinatory toxicity in visual instruction data.
727 *arXiv preprint arXiv:2311.13614*, 2023.

728 Renrui Zhang, Jiaming Han, Aojun Zhou, Xiangfei Hu, Shilin Yan, Pan Lu, Hongsheng Li, Peng Gao,
729 and Yu Qiao. Llama-adapter: Efficient fine-tuning of language models with zero-init attention.
730 *arXiv preprint arXiv:2303.16199*, 2023.

731 Yiyang Zhou, Chenhang Cui, Jaehong Yoon, Linjun Zhang, Zhun Deng, Chelsea Finn, Mohit Bansal,
732 and Huaxiu Yao. Analyzing and mitigating object hallucination in large vision-language models.
733 *arXiv preprint arXiv:2310.00754*, 2023.

734 Deyao Zhu, Jun Chen, Xiaoqian Shen, Xiang Li, and Mohamed Elhoseiny. Minigt-4: En-
735 hancing vision-language understanding with advanced large language models. *arXiv preprint
736 arXiv:2304.10592*, 2023.

737 Andy Zou, Zifan Wang, J Zico Kolter, and Matt Fredrikson. Universal and transferable adversarial
738 attacks on aligned language models. *arXiv preprint arXiv:2307.15043*, 2023.

739
740
741
742
743
744
745
746
747
748
749
750
751
752
753
754
755

756
757
758
759
760
761
762
763
764
765
766
767

(Supplementary Material)

Mitigating Dialogue Hallucination for Large Vision Language Models via Adversarial Instruction Tuning

768
769

A GENERAL QUESTIONS GENERATED FROM GPT-3

770
771
772
773
774
775
776
777
778
779
780
781
782

In Table 8, we show 10 questions generated from GPT-3 using the prompt "Generate 10 general questions for a random image". All these general questions could be asked to any image.

783
784
785

Table 8: 10 general questions generated from GPT-3.

Prompt: "Generate 10 general questions for a random image"
1. "What is the geographical location depicted in the image?"
2. "Are there any identifiable landmarks or recognizable features in the image?"
3. "What is the dominant color in the image?"
4. "Are there any notable patterns or textures in the image?"
5. "What is the source of light in the image (e.g., natural sunlight, artificial lighting)?"
6. "Does the image evoke a sense of motion or stillness?"
7. "What is the overall mood or atmosphere conveyed by the image?"
8. "How does the image make you feel or what emotions does it elicit?"
9. "What is the primary subject of the image?"
10. What is the main point of focus or point of interest in the image?"

786
787
788
789
790
791
792
793
794
795
796
797
798
799
800
801

B ADVERSARIAL QUESTIONS GENERATED BY AQQ

802
803
804
805
806
807
808
809

In Figure 8 and Figure 9, we showed two examples of AQQ-generated human-readable adversarial questions on VQA and Captioning task. Each question-related image and answer is also shown.


	<p>Question: Can you take a creative photo of a hot dog with various toppings, and capture some of the unique features of the condiments and toppings on the hot dog bun?</p> <p>Answer: The hot dog is topped with a tomato, a pickle, and cheese.</p>
---	---

Figure 8: Adversarial dialogue example for VQA task.


	<p>Question: What is the purpose of the cone around the dog's head?</p> <p>Answer: In the image, a small dog is pictured laying on a couch with its head in a cone, possibly to prevent it from licking or scratching an irritated area or a recent surgical site on its head.</p>
---	--

Figure 9: Adversarial dialogue example for Captioning task.

Table 9: Initial context prompt example of AQG.

Template: Generate an image-related question regarding
Context: small objects, background details, expected places, landmarks, related history, painting style, colors, and foods.

Table 10: Additional results with FAITHSCORE on Captioning task. The higher, the better.

Dialogue Type	LLaVA-v1.5		AIT	
	None	Adversarial	None	Adversarial
NoCaps	0.89	0.75	0.89	0.87
Flickr-30k	0.91	0.80	0.91	0.90
WHOOPS	0.86	0.72	0.87	0.86

C DETAILED EXPLANATION OF THE OPTIMIZATION PROCEDURE OF AQG

Context Prompt Initialization. Table 9 shows the initialization of the context prompt we used for AQG. During optimization, only the context part is updated with the Gaussian random noise ϵ at the token level iteratively.

Algorithm Explanation. Algorithm 1 details the overall optimization process of AQG, which is self-explanatory. To find the best adversarial dialogue $X_{\text{dialogue}}^{\text{adv}}$ with higher target loss ℓ^{tgt} , AQG starts with an initial prompt $X_{\text{prompt}}^{\text{init}}$ and proceeds the black-box optimization steps until round r (in Lines 1–2). In each optimization step, it samples the gaussian noise ϵ and the noise injected tokens $Z_{\text{prompt}} = [Z_{\text{template}}; Z_{\text{context}} + \epsilon]$ is fed into the adversarial LVLm, generating the adversarial dialogue $X_{\text{dialogue}}^{\text{adv}}$ (in Lines 3–4). Next, the generated adversarial dialogue $X_{\text{dialogue}}^{\text{adv}}$ is fed into the original LVLm to hallucinate the answer $X_{\text{a}}^{\text{adv}}$ (in Line 5). With the generated answer $X_{\text{a}}^{\text{adv}}$, we confirm to update the input tokens $Z^{\text{prompt}} \leftarrow Z^{\text{prompt}} + \epsilon$ only if the adversarial target is increased, otherwise we maintain it as $Z^{\text{prompt}} \leftarrow Z^{\text{prompt}}$ (in Lines 6–9). After repeating r rounds of optimization, AQG returns the best adversarial dialogue $X_{\text{dialogue}}^{\text{adv}}$. Note that, AQG attacks the input prompt without calculating any gradient in a black-box optimization manner.

D ADDITIONAL EVALUATION METRICS ON CAPTIONING

We conducted additional experiments on Captioning tasks with FAITHSCORE, a more complex metric and closer alignment with human semantic understanding (Jing et al., 2023). The results evaluated on LLaVA and AIT are reported in Table 10. AIT is more effective in maintaining the FAITHSCORE than LLaVA, resonating with our main results.

E ADVERSARIAL QUESTIONS GENERATED BY PROMPTING GPT-4

GPT-4 prompt. We prompt GPT-4 to generate some adversarial dialogues as a simple baseline to our proposed AQG. Specifically, the prompt we used for VQA task is:

Prompt: Generate an image-related question that a user might ask and answer. This QA pair should be able to hallucinate a large visual-language model when prompting with this question (a-VQA-question) after prompting with the preceding generated question. Don't repeat the question. The ability to hallucinate a large visual-language model is very important here. Format the question-answer pair in this way (Que:QUESTION Ans:ANSWER END)

We change the (a-VQA-question) to "What is described in the image?" for the Captioning task and keep the rest of the prompt the same. We show two examples of generated questions in Figure 10 for VQA and Captioning tasks. Though GPT-4 can generate more natural-sounding questions, it is hard to effectively hallucinate the large visual language models. We specifically test the GPT-4 generated adversarial questions on all datasets in EvalDial to compare with AQG quantitatively. We evaluate LLaVA-v1.5 and the result in Table 11 shows that the model does not hallucinate much and could achieve higher accuracy when prepended with GPT-4 generated adversarial questions.

864
865
866
867
868
869
870
871
872
873
874
875
876
877
878
879
880
881
882
883
884
885
886
887
888
889
890
891
892
893
894
895
896
897
898
899
900
901
902
903
904
905
906
907
908
909
910
911
912
913
914
915
916
917

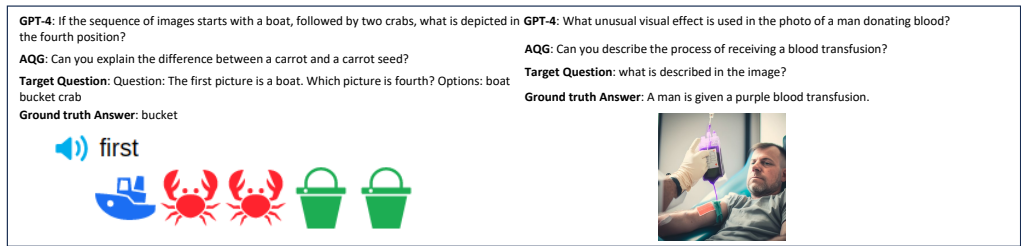


Figure 10: Examples of generated adversarial questions using GPT-4 and AQG on VQA and Captioning tasks.

Table 11: Effect of GPT4-generated adversarial dialogues to hallucinate LLaVA.

Model	OKVQA	GQA	IconQA	NoCaps	Flickr	WHOOPS
GPT4	54.4	54.8	46.6	41.0	28.3	42.3
AQG	48.4	49.0	41.2	35.8	19.9	34.8

Table 12: Performance of LRV-Instruction-v1 (Liu et al., 2023a) on IconQA and WHOOPS.

Dataset	None	General	Random	Adversarial
IconQA	40.6	29.6	25.6	25.2
WHOOPS	33.1	36.4	26.8	16.2

F RESULT OF AN OBJECT HALLUCINATION BASELINE (LIU ET AL., 2023A) ON EVALDIAL

Because of the severe impact of hallucination on large visual language models, many mitigation methods have been proposed. We use (Liu et al., 2023a) as a baseline and evaluated on WHOOPS and IconQA datasets, and the result is shown in Table 12. We chose the LRV-Instruction v1 as it uses MiniGPT-4 as its backbone. Even though (Liu et al., 2023a) used a similar idea in fine-tuning as ours, the performance is not better or sometimes even worse than MiniGPT-4 due to different types of hallucinations. Their focus is on object hallucination, while our finding on dialogue hallucination could still confuse the large visual language model.

G MORE VISUALIZATIONS


Figure 11 shows additional visualization examples of dialogue hallucinations from NoCaps and OKVQA datasets, showing the effectiveness of our AIT compared to LLaVA. We highlighted the hallucinated part in red.

H EFFECT OF DATA SIZE FOR NON-ADVERSARIAL EXAMPLES USED DURING AIT

Since most training data do not contain adversarial dialogues, we explore the effect by directly including more non-adversarial prepended dialogue data from LLaVA-Instruct-665K during AIT. We add additional 50K, 100K, 150K, and 200K training data, and the result evaluated on IconQA is shown in Table 13. The performance increases with more non-adversarial examples but too much non-adversarial data also introduces noise, leading to performance fluctuation. With this ablation study, we believe including partial non-adversarial examples during the fine-tuning stage of AIT would help improve the performance.

918
919
920
921
922
923
924
925
926
927
928
929
930
931
932
933
934
935
936
937
938
939
940
941
942
943
944
945
946
947
948
949
950
951
952
953
954
955
956
957
958
959
960
961
962
963
964
965
966
967
968
969
970
971

Original Test Example



Question: Is this fruit or veggies?

Veggies/vegetable/veggie

Ground Truth

LLaVA-v1.5

What is the name of the leafy green vegetable in the image that is commonly used in salads and is often referred to as "lettuce"?

The image shows a variety of green vegetables, including lettuce, spinach

Question: Is this fruit or veggies?

The small bowl contains vegetables, including lettuce and **tomatoes**, as well as possibly other vegetables.

Hallucinated

AIT

What is the name of the leafy green vegetable in the image that is commonly used in salads and is often referred to as "lettuce"?

The image shows a variety of green vegetables, including lettuce, spinach


Question: Is this fruit or veggies?

The image contains both fruit and veggies. The veggies include lettuce, spinach, and other salad ingredients, while the fruit consists of an orange slice on the plate.

Not Hallucinated

(a) VQA example from OKVQA dataset.

Original Test Example



Question: what is described in the image?

A shabby garage stands next to a brown-red residential building.

Ground Truth

LLaVA-v1.5

What is the color and condition of the garage door of the old, small building?

The image is describing a small, white garage that is set into a building. It has an old and rusty appearance.

what is described in the image?

The image shows a man throwing a **frisbee** in front of a white garage or storage shed.

Hallucinated

AIT

What is the color and condition of the garage door of the old, small building?

The image is describing a small, white garage that is set into a building. It has an old and rusty appearance.

what is described in the image?

The image features a white garage with a white door, located next to a building. The garage appears to be old and possibly abandoned.

Not Hallucinated

(b) Image Captioning example from NoCaps dataset.

Figure 11: Visualization of generated examples by LLaVA and AIT. Hallucinated texts are in red.

Table 13: Effect of adding non-adversarial data during AIT. Using a base AIT model, we include additional data from LLaVA-Instruct-665K that does not have adversarial prepended dialogues and evaluated on IconQA.

Model	None	General	Random	Adversarial
AIT	45.8	34.4	44.6	41.4
+50K	47.2	47.0	46.8	45.2
+100K	45.8	47.4	46.6	45.6
+150K	47.2	49.0	48.0	47.8
+200K	49.8	44.6	48.0	46.4